With Eq. (A6), the expression (A3) can now be written as

$$I_n = \frac{(-1)^{2-n}}{4-n} \int_{-\infty}^{\infty} \frac{(\pi^2 + x^2) x^2 dx}{(1 + e^{-x})^2}, \quad n = 1, 2. \quad \text{(A7)}$$

By employing the hyperbolic cosine and Gradshteyn and Ryzhik's formula (3.527.5), the integral in Eq.

(A7) is readily evaluated:

$$I_n = \frac{(-1)^{2-n}}{4-n}(\tfrac{4}{5}\pi^4). \quad \text{(A8)}$$

Hence, from (A2) and (A8) the final value of I_b is seen to be $2\pi^4/15$.

Absolute X-Ray Measurement of the Atomic Scattering Factor of Nickel

M. Diana and G. Mazzone*

Laboratorio Fisica Nucleare Applicata, C.S.N. Casaccia, 00100, Roma, Italia

AND

J. J. DeMarco

Army Materials and Mechanics Research Center, Watertown, Massachusetts 02172

(Received 13 March 1969)

Joint measurements were made at Laboratorio F.N.A. Casaccia, Rome, Italy and at AMMRC, Watertown, Mass. to determine the atomic scattering factor of nickel. These studies were made using imperfect single crystals in transmission and applying a measured secondary extinction correction to the integrated intensities obtained with Mo $K\alpha$ and Ag $K\alpha$ radiation. A measurement of the incident beam power placed the measurements on an absolute scale. Three crystals were studied whose thicknesses T were 31, 44, and 59 μ. Unlike similar measurements on aluminum by DeMarco, the apparent atomic scattering factors of nickel were found to depend on the reflection half-width Δ, thus indicating the presence of primary extinction. By comparing the measured scattering factors as a function of T^2/Δ^2, the dependence was found to be linear with a slope proportional to the square of the wavelength up to a difference of approximately 6% between extrapolated and observed scattering factors. The atomic scattering factors for the (111) and (200) reflections determined from an extrapolation to $T^2/\Delta^2 = 0$ are found to be considerably lower than the theoretical value for the $3d^8 4s^2$ configuration.

INTRODUCTION

MAGNETIC form factors for $3d$ electrons in iron, cobalt, and nickel have been measured by Shull and co-workers[1] resulting in a good degree of compatibility with free-atom calculations. This seems to indicate that in these metals there is no significant variation in the electron distribution due to bonding effects, at least at the top of the $3d$ band. Because of the form of the electron wave functions at the top of the band the magnetic scattering factors from band calculations are not expected to be very different from those obtained from a free-atom approximation. It is therefore necessary to perform atomic scattering factor measurements with high accuracy to ascertain possible differences between theoretical and experimental results. X-ray atomic scattering factors have been measured for chromium,[2,3]

iron,[4,5] copper,[5–8] and nickel[9–11] in which conflicting values have been reported. Although each measurement is reported to a high degree of accuracy, the values of the atomic scattering factors range from agreement with to 3–4% less than theoretical values. With the exception of measurements on nearly perfect crystals of copper,[6] all of the cited studies were on powders. In an attempt to clarify the experimental situation, we have measured the atomic scattering factor of nickel exploiting a different technique. Nickel was chosen because it was found that suitably thin samples could be easily prepared.

To perform accurate and reliable intensity measurements on single crystals, a method has been recently

* Present address: Servizio Organizzazione E Metodi, Comitato Nazionale per l'Energia Nucleare Viale R. Margherita 125, 00100, Roma, Italy.
[1] C. G. Shull and Y. Yamada, J. Phys. Soc. Japan **17**, Suppl. BIII, 1 (1962); R. M. Moon, Phys. Rev. **136**, A195 (1964); H. A. Mook, *ibid.* **148**, 495 (1966).
[2] M. J. Cooper, Phil. Mag. **7**, 2059 (1962).
[3] S. Hosoya, J. Phys. Soc. Japan **19**, 235 (1964).

[4] T. Paakkari and P. Suortti, Acta Cryst. **22**, 755 (1967).
[5] B. W. Batterman, D. R. Chipman, and J. J. DeMarco, Phys. Rev. **122**, 68 (1961).
[6] L. D. Jennings, D. R. Chipman, and J. J. DeMarco, Phys. Rev. **135**, A1612 (1964).
[7] S. Hosoya and T. Yamagishi, J. Phys. Soc. Japan **21**, 2638 (1966).
[8] M. Linkoaho, E. Rantavuori, and U. Korhonen, Ann. Acad. Sci. Fennicae: Ser. A. **VI**, 219 (1967).
[9] O. Inkinen and P. Suortti, Ann. Acad. Sci. Fennicae: Ser. A. **VI**, 147 (1964).
[10] S. Hosoya (unpublished).
[11] P. M. Raccah (unpublished).

reported which permits one to obtain scattering factor values free from secondary extinction and to assess the amount of primary extinction. This method, already applied to aluminum[12] and magnesium[13] single crystals, enables one to avoid some of the uncertainties which seem to be inherent in powder measurements. In essence, one measures integrated intensities in transmission from a very thin crystal using a narrow beam whose divergence is the order of a few minutes of arc. By simultaneously measuring the transmitted and diffracted power as the crystal is rocked through the reflection, it is possible to have a point by point correction for secondary extinction. To assess the amount of primary extinction, the scattering factor values obtained from different spots of the crystal are examined as a function of the reciprocal half-width squared. From an extrapolation to infinite half-width the effects of primary extinction can then be removed. This extrapolation may be justified the following way: The point by point correction for secondary extinction is not based upon any particular mosaic distribution and, therefore, in the absence of primary extinction there will be no dependence of scattering factor on the peak half-width.[12] If, however, a small amount of primary extinction is present, it may manifest itself as the reflection half-width gets smaller. It is known that extinction depends on the square of the radiation wavelength and on the square of the thickness of the mosaic blocks. If this thickness was known, one could extrapolate linearly to zero thickness the square of the scattering factors against the average of the thickness squared and obtain a result free from primary extinction. If, however, the scattering factors have to be extrapolated from a plot in which the abscissa is the square of the reciprocal of the peak half-width, it is not possible to foresee what would be the analytical form of the extrapolation, since the dependence of mosaic block thickness on half-width is not known. If certain mathematical conditions were met, one could think of writing the average of the thickness squared $\langle t_0{}^2 \rangle_{av}$ as a series expansion of the square of the reciprocal half-width

$$\langle t_0{}^2 \rangle_{av} = \sum_n a_n (1/\Delta^2)^n . \qquad (1)$$

For small reciprocal half-width one could disregard all high-order terms and retain just the first-order term so that

$$\langle t_0{}^2 \rangle_{av} = a_1 (1/\Delta^2) . \qquad (2)$$

In this case, then, the extrapolation of the square of the scattering factors versus the square of the reciprocal half-width should be linear. There is, of course, no reason to admit this is the case. Only when the squares of the scattering factors have actually been plotted against $(1/\Delta)^2$ is it possible to judge to what extent they vary linearly and then perform the extrapolation. In any

case, if one has a sufficient number of scattering factors derived from reflections with large half-widths, then the exact form of the extrapolation is not going to significantly affect the result. In fact, for infinite half-width the mosaic blocks are of infinitesimal size, so that no correction for primary extinction is necessary. In addition the measurements can be repeated using a radiation having a different wavelength. Because of λ^2 dependence of primary and secondary extinction in the Laue case, it is possible to check the validity of the extrapolation procedure.

EXPERIMENT

Three nickel single crystals of 99.99% purity grown from the melt were spark-planed and then ground to provide three slabs approximately 31, 44, and 59 μ thick, whose surfaces were parallel to the (110) plane to within 2°. The crystals were examined by a series of transmission and back reflection Laue photographs taken over several locations on their faces. They were also scanned over various crystal zones to determine the possible presence of polycrystalline layers. The measurements performed at Casaccia were made using the Mo $K\alpha$ radiation monochromated by a singly bent LiF crystal. The x-ray tube was operated between 40 and 44 kV to reduce the amount of second-order contamination. The amount of $\lambda/2$ component present in the diffracted beam was the order of 0.1% and completely eliminated by the use of pulse-height discrimination. The incident beam consisted of α_1 and α_2 wavelengths in the ratio of approximately 3:1. By the use of two pinholes the incident beam divergence was collimated to 2.5 min of arc, a factor of 5 less than the smallest half-width observed, and having a cross section of approximately 10^{-1} mm^2 at the sample surface. The reflections (111), (200), (220), and (400) of nickel were measured with an incident beam power in the order of 7500 cps with a total circuitry dead time of 2 μsec. For the measurements of the high-angle reflections (333), (511), (600), and (800), a much stronger beam was used, whose incident intensity was measured by means of a series of Zr absorbers. The uncertainty in the absolute values for these high-angle scattering factors due to the use of attenuators was determined to be $\frac{1}{2}$%.

Two fixed counters were used simultaneously, such that one measured the diffracted intensity while the other recorded the transmitted beam. The counters had been examined and their efficiency found to be constant over the entire surface of the scintillating crystals. To place the measurements on an absolute basis the incident beam was measured by the counter that recorded the diffracted intensity. This eliminated the necessity of determining the relative efficiency of the two counters. By removing the crystal from the path of the incident beam, the absorption factor of the crystal was measured.

To correct for secondary extinction, use was made

[12] J. J. DeMarco, Phil. Mag. **15**, 483 (1967).
[13] R. J. Weiss, Phil. Mag. **16**, 141 (1967).

of the following relations[12,14]:

$$P_H = \frac{P_H{}^*P_T}{P_T{}^*} + \frac{P_H{}^*}{3}\left[\frac{P_T}{P_T{}^*} - 1\right]^2, \quad (3)$$

where $P_H{}^*$ and P_H are the instantaneous diffracted powers with and without secondary extinction and $P_T{}^*$ and P_T, the corresponding transmitted power. To account for the finite beam divergence, the integrated intensities derived from Eq. (3) were modified in the following way:

$$\int P_H dy = \int \frac{P_H{}^*P_T}{P_T{}^*} dy$$
$$+ \left(\frac{\Delta m}{\Delta} - 1\right)\left[\int \frac{P_H{}^*P_T}{P_T{}^*} dy - \int P_H{}^* dy\right], \quad (4)$$

where Δ_m is the observed half-width of the peak and Δ is the half-width of the mosaic distribution function. The correction for secondary extinction was therefore made by increasing each element of diffracted intensity $P_H{}^*$ measured at angular intervals of 3 min of arc 2θ, by the ratio $P_T/P_T{}^*$. For a few points at the top of the peak, the second-order term appearing in Eq. (3) was also added. The ratio of the corrected to uncorrected integrated intensities after background subtraction is the correction for secondary extinction. This correction was applied to the integrated intensity minus background of the same reflection measured by a continuous scan. By rotating the crystal 180° and averaging the results, the first-order effects due to miscut were avoided. Second-order effects were approximately 0.1% and therefore neglected. The total statistical error in the integrated intensities, the secondary extinction correction, and the incident intensity measurement was calculated to be the order of 1%. At low angles the thermal diffuse scattering (TDS) correction was small (see Table I), so that systematic errors of any consequence could arise only from the absorption coefficient of nickel, which was measured to be 4.15.7±5 cm^{-1} for molybdenum $K\alpha$ radiation and 215.9±2 cm^{-1} for silver $K\alpha$ radiation. By observing the transmitted beam and having the freedom to rotate the crystal in a plane normal to the diffracting vector, it is possible to avoid additional reflections taking place in the angular range of the reflection being measured. A study of the TDS and Debye temperature factor was made using a thick single crystal of nickel in Bragg reflection. The crystal was prepared from the same boule which provided the three thin crystal slabs used to measure the low-angle reflections. A test of the Nilsson TDS correction[15] was made by observing the integrated intensity given from the (600) reflection as a function of the angular deviation from the peak. In this manner the accuracy of the

Nilsson formulation was assessed to be within 10% of itself. By measuring the (800) plane in Bragg reflection on an absolute basis and using the theoretical value of the atomic scattering factor[16] along with the Nilsson TDS correction, the Debye temperature Θ was determined to be $(390\pm5)°$K. The resulting Debye-Waller parameter $B=0.397\pm0.010$ compares favorably with a calculated value[17] of $B=0.381\pm0.008$ obtained from a detailed description of the phonon states.

The atomic scattering factor for the nickel (111) reflection was remeasured at AMMRC, Watertown, Mass. using the thinnest (31-μ) and the thickest (59-μ) crystals with molybdenum $K\alpha$ and silver $K\alpha$ radiations. These measurements were made in the same manner as has been described for the studies performed at Casaccia, Rome. The experimental conditions at the Mo $K\alpha$ and Ag $K\alpha$ wavelengths were essentially identical having only slight differences in the incident beam divergence, the total count rate and the dead-time correction. With the Mo $K\alpha$ wavelength the divergence of the incident beam was 1.8 min of arc with a maximum count rate of 4300 cps at a power setting of 50 kV and 20 mA. With Ag $K\alpha$ wavelength the beam divergence was 2.2 min of arc with a count rate of 3800 cps. The maximum circuitry dead-time correction in both cases was the order of 2%. For both wavelengths the $\lambda/2$ component diffracting from a LiF singly bent monochromator amounted to 0.3–0.5%, which was easily eliminated by energy discrimination. The incident beam in each case consisted of α_1 and α_2 wavelengths within 2% of their natural ratio.

RESULTS

The measured values of $(f+\Delta f')^2 + (\Delta f'')^2$ for the three principal reflections of nickel are shown in Figs. 1–3. These values have been adjusted by a measured secondary extinction correction that ranged from 15 to 1% for the measurements at the Mo $K\alpha$ wavelength, and from 7 to 1% for those obtained with Ag $K\alpha$ wavelength (see Table I). If primary extinction is operative, it is expected that $(f+\Delta f')^2 + (\Delta f'')^2$ will be reduced by the factor[18]

$$[1 - A^2/3 + \cdots], \quad (5)$$

where

$$A = \frac{e^2 \lambda N |F| K t_0 e^{-m}}{mc^2 \gamma_0}. \quad (6)$$

The terms that define A are e^2/mc^2 the classical electron radius, N the number of unit cells per unit volume, λ the radiation wavelength, K the polarization factor, e^{-m} the temperature factor, F the crystal structure factor, and γ_0 the direction cosine between the incident (or reflected) radiation direction and the crystal's sur-

[14] J. J. DeMarco, M. Diana, and G. Mazzone, Phil. Mag. 16, 1303 (1967).
[15] N. Nilsson, Arkiv Fysik 12, 247 (1957).

[16] A. J. Freeman and R. E. Watson, Acta Cryst. 14, 231 (1961); R. E. Watson and A. J. Freeman, ibid. 14, 27 (1961).
[17] H. W. T. Barron and T. Smith, J. Chem. Solids 27, 1951 (1966).
[18] R. J. Weiss, X-ray Determination of Electron Distributions (North-Holland Publishing Co., Amsterdam, 1966), p. 48.
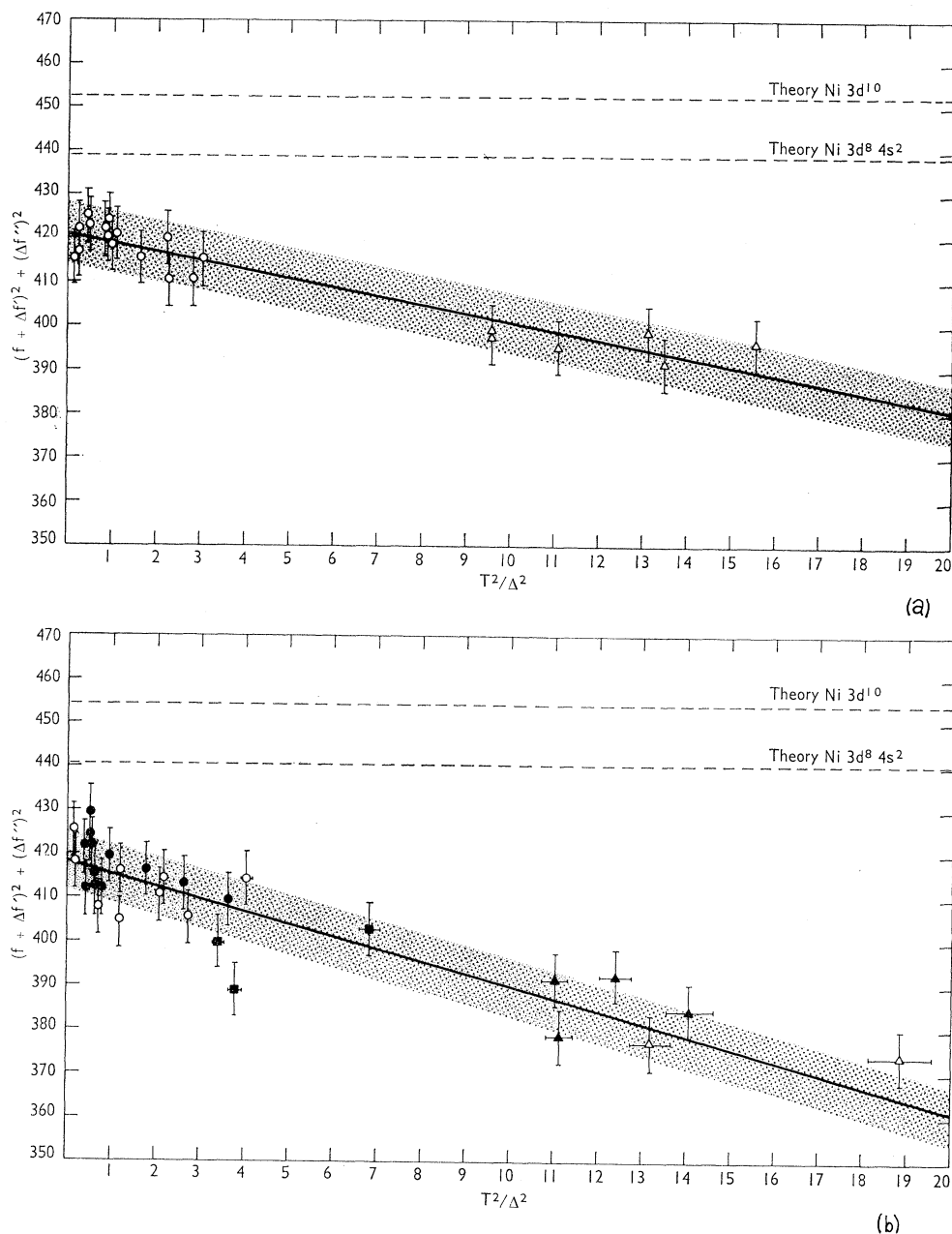
FIG. 1. The atomic scattering factors measured from the (111) reflection of nickel with (a) Ag $K\alpha$ wavelength and (b) Mo $K\alpha$ wave length are shown as a function of T^2/Δ^2. The symbols ●, ■, and ▲ denote the values obtained from crystals of thicknesses 31, 44, and 59 μ, respectively. The open symbols refer to measurements made at AMMRC, Watertown, Mass. All values shown have been corrected for secondary extinction. The best least-square straight-line fit for all values is shown by a solid line enclosed by a shaded band indicating the limits of error. To determine the linear extrapolation for the data obtained with Mo $K\alpha$ wavelength (b), the results from the thickest crystal were decreased from 0.4 to 0.9% due to the effect of higher-order terms in the primary extinction correction.

face. Since we do not know t_0 the size of the mosaic blocks, and since it is expected that primary extinction will decrease with increasing half-width and decreasing crystal thickness, we have chosen to observe $(f+\Delta f')^2+(\Delta f'')^2$ as a function of T^2/Δ^2. If the reflection half-width Δ is proportional to the number of perfect crystal blocks N of size t_0 in a crystal of thickness T, then T^2/Δ^2 becomes proportional to A^2. For this case, the

primary extinction correction to first order is linear. As the effect of primary extinction increases, the higher-order terms in the primary extinction correction become important and the behavior of $(f+\Delta f')^2+(\Delta f'')^2$ with A^2 departs from linearity. It is further expected that in observing $(f+\Delta f')^2+(\Delta f'')^2$ measured with molybdenum radiation and with silver radiation the reduction of primary extinction should be in the ratio of the wave-
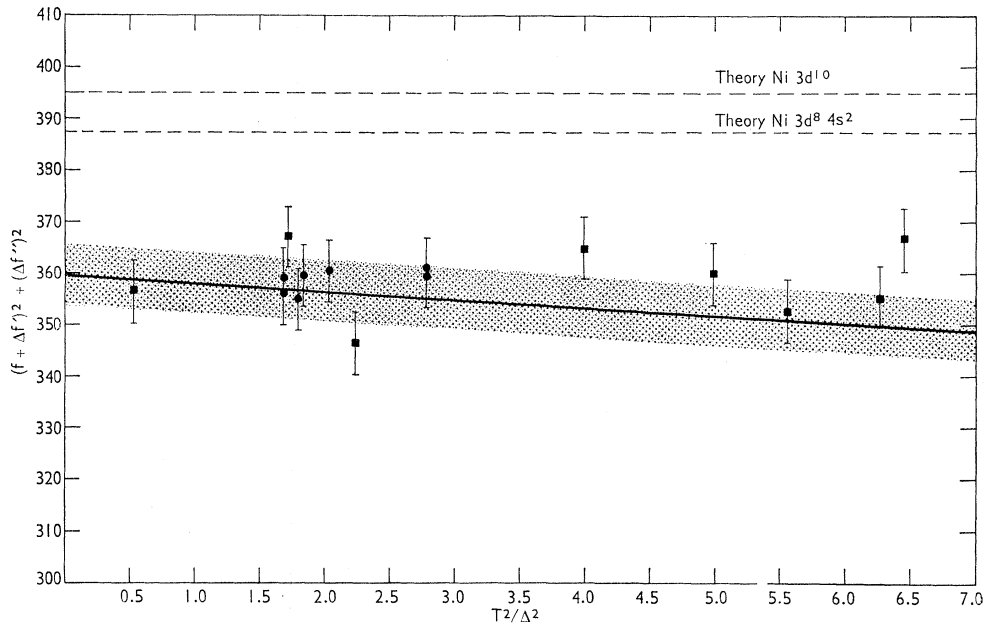
Fig. 2. The atomic scattering factors measured from the (200) reflection of nickel with molybdenum radiation are shown as a function of T^2/Δ^2. The symbols have the same significance as in Fig. 1. All values have been corrected for secondary extinction and their mean value has been assigned as the intercept. The slope of the solid line through the intercept has been determined from the behavior of primary extinction observed for the (111) reflection, assuming that t_0 is uniform in all directions. The standard error is shown by the shaded band.
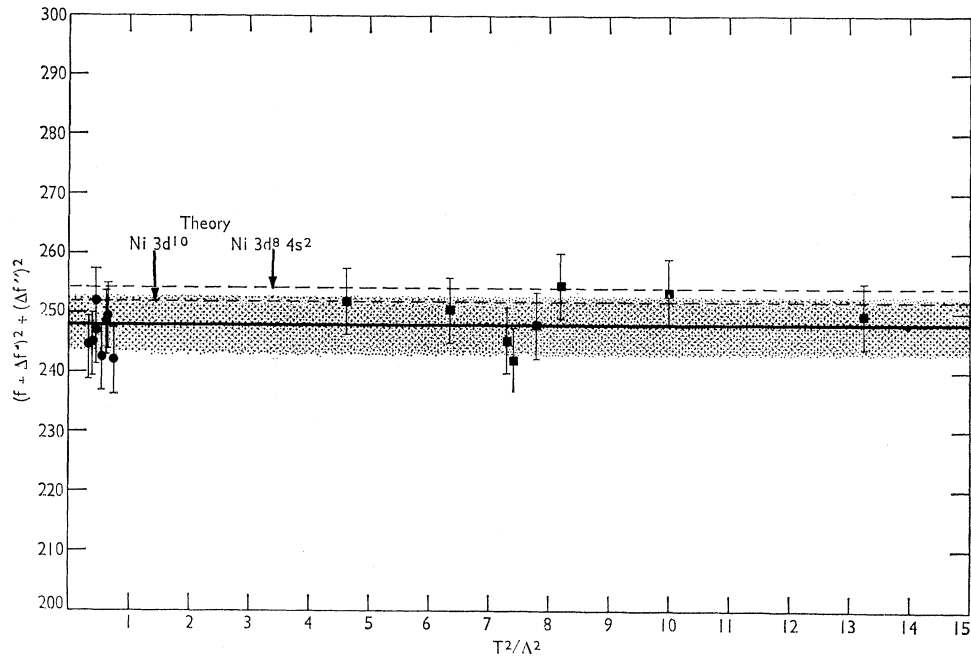

Fig. 3. The atomic scattering factors measured from the (220) reflection of nickel with molybdenum radiation are shown as a function of T^2/Δ^2. The symbols have the same significance as in Fig. 1. All values have been corrected for secondary extinction and their mean value is indicated by a solid line. The shaded band indicates the standard error.

lengths squared. Our results for the (111) are not independent of T^2/Δ^2 and we have assumed this to be due to primary extinction.

Analyzing the results for the (111) reflection we have evaluated the best least-square straight-line fit to the data taken with silver radiation, since it appeared to be linear within the range of measured value [Fig. 1(a)]. This has indicated a linear dependence on T^2/Δ^2 up to a departure of approximately 6% from the intercept value. The magnitude of primary extinction in the

TABLE I. The thermal diffuse scattering correction and the range of secondary extinction correction measured for the nickel crystal with molybdenum radiation.

hkl	%TDS	%secondary extinction
(111)	0.24[a]	1.6– 7.4[a]
	0.24–0.59[b]	1.9–14.8
(200)	0.29–0.62[b]	3.7– 9.9
(220)	0.71–1.20[b]	1.1– 4.3
(400)	2.19	0.6
(333)–(511)	4.48	0.5 estimated
(600)	4.92–9.08[b]	
(800)	8.40–9.80[b]	

[a] Silver radiation.
[b] Depending on the angular range of scan.

measurements taken with molybdenum radiation ranged to approximately 13% [Fig. 1(b)]. In order to perform a linear extrapolation, we have corrected those results exhibiting primary extinction greater than 6%, for the effect of higher-order terms in the primary extinction correction. This amounted to a 0.4–0.9% decrease for the results obtained from the thickest crystal. A least-square straight-line fit was then computed for all values, measured with molybdenum radiation. By extrapolating to zero thickness in both cases we have determined extinction free values of $(f+\Delta f')^2 + (\Delta f'')^2$ that are in agreement within 0.7%. The slopes of the linear extrapolation for silver and molybdenum radiation are in the ratio of 1.41. With each slope having an accuracy of $\pm 10\%$, the ratio of the slopes are in agreement with the ratio of the wavelengths squared (1.61). A separate analysis of the sets of data taken at Laboratorio FNA, Casaccia, Rome and at AMMRC, Watertown, Mass. with molybdenum radiation yielded intercepts and slopes within $\pm 0.5\%$ of each other. In considering the thin-crystal (31-μ) data from both laboratories, separately and together, the best least-square straight-line fit was found to be compatible, within the limits of error, with the data obtained from both the

intermediate (44-μ) and thickest crystal. Regardless of how one assesses the data, the intercept is affected only by a few tenths of one percent at most.

The standard error for each observation (shown by error bars) has been determined from the square root of the sum of the deviations of each point about the least-square straight line. In every case, this error was found to be several tenths of a percent larger than the standard error evaluated from counting statistics only. While the error on T^2/Δ^2 was estimated to be the order of $\pm 3\%$, its effect on both the intercept and slope is considered negligible.

Listed in Table II are the atomic scattering factor values determined from the extrapolation to $T^2/\Delta^2 = 0$. The dispersion corrections used to obtain f are those of Cromer.[19] The standard error assigned to each value has been determined from an assessment of all parameters involved in the measurements, of which the uncertainty of the absorption coefficient ($\pm 1\%$) is the largest contributing factor. The intercept value of $(f+\Delta f')^2 + (\Delta f'')^2$ for the (111) reflection measured with Ag $K\alpha$ radiation is 0.7% higher than that measured with Mo $K\alpha$ radiation. Since these values lie within our limits of error, we have averaged the two values and compared the result with theory.[16]

The data for all reflections have been assessed in the same manner. However, the error in the slope of the least-square straight-line fit for the (200) and (220) data (Figs. 2 and 3) is large enough to be consistent with the slope being zero. For this reason the intercepts for these reflections have been obtained by averaging their respective values of $(f+\Delta f')^2 + (\Delta f'')^2$. If t_0 is the same in all directions then the slope of the line through the intercept for the (200) reflection is predicted by the slope of the line obtained for the (111) reflection. This has been determined by evaluating the reduction in primary extinction due to the factors K, $|F|$, e^{-m}, and

TABLE II. Atomic scattering factors of nickel. The atomic scattering factor listed for the (111) reflection has been determined from the mean result of $(f+\Delta f')^2 + (\Delta f'')^2 = 421.04 \pm 6.74$ (measured with silver radiation) and 418.26 ± 6.69 (measured with molybdenum radiation). While atomic scattering factors have yet to be determined from available band calculations,[a] we have contrasted our results with those predicted by Hartree-Fock free-atom calculation for both the $3d^{10}$ and the $3d^8 4s^2$ configurations. It is important to note that neutron results suggest a $3d^{9.4} 4s^{0.6}$ configuration. The experimental and calculated parameters involved in evaluating the measured atomic scattering factors are

λ	μ	$\Delta f'$	$\Delta f''$
0.560834 Å	215.91±2	0.35	0.80
0.71069 Å	415.7 ±5	0.37	1.20
	$a_0 = 3.524$ Å	$B = 0.397 \pm 0.010$	

(hkl)	f_{crystal}	$f_{\text{theory}}{}^{3d^8 4s^2}$	$f_{\text{theory}}{}^{3d^{10}}$	$f_{\text{theory}}{}^{3d^8 4s^2}/f_{\text{crystal}}$	$f_{\text{theory}}{}^{3d^{10}}/f_{\text{crystal}}$
(111)	20.10±0.16	20.59	20.91	1.024±0.008	1.040±0.008
(200)	18.55±0.16	19.28	19.47	1.039±0.009	1.050±0.009
(220)	15.34±0.12	15.53	15.47	1.012±0.008	1.008±0.008
(400)	11.18±0.11	11.46	11.39	1.025±0.010	1.019±0.010
(511)	8.73±0.09	8.88	8.85	1.017±0.010	1.014±0.010
(333)	8.74±0.09	8.88	8.85	1.016±0.010	1.013±0.010
(600)		7.85	7.84		
(800)		6.33	6.33		

[a] J. W. D. Connolly, Phys. Rev. **159**, 415 (1967).

[19] D. T. Cromer, Acta Cryst. **18**, 17 (1965).

γ_0 in Eq. (6) and has been drawn in Fig. 2 for comparison with actual data.

For the (400) reflection, four measurements of $(f+\Delta f')^2+(\Delta f'')^2$ were made with the thinnest crystal and two with the crystal of intermediate thickness (44 μ). These results are averaged to give the value listed in Table II. The measured atomic scattering factor listed for the (511) and the (333) reflections result from an averaging of ten measurements each on the thin crystal.

It is interesting to note the similiarity between the measured form factors of nickel and aluminum.[12] For both fcc metals, the form factor for the first two reflections are lower than theory with the scattering factor of the (200) reflection having the largest discrepancy. In both cases, the scattering factor of the (511) and (333) reflections indicate that the core charge distribu-

tion is spherically symmetric. Combining this with the observation that the (400) form factor of nickel is also low, leads one to suspect the possibility that the outer electrons are spread out along directions that have the smallest atomic density. It would therefore be interesting to perform measurements of atomic scattering factors in metals with different crystal symmetry and to compare the results with theoretical data obtained from accurate band calculations.

ACKNOWLEDGMENTS

Helicon-Acoustic Dispersion Relations in Metals: Effective-Mass and Relaxation-Time Dependence*†

G. Persky‡ AND T. Kjeldaas, Jr.

Department of Physics Polytechnic Institute of Brooklyn, Brooklyn, New York 11201

(Received 19 May 1969)

The electromagnetic, constitutive, and lattice equations governing propagation of transverse acoustic and electromagnetic waves in a metal with conduction electrons possessing a constant scalar effective mass, and in which there is a uniform magnetic field applied along the propagation direction, are given. These equations are used to derive a secular equation describing the dispersion of interacting helicon and acoustic waves, and in which additional structure arising from the difference between the free-electron mass and the effective electron mass is evident. Magnetoacoustic attenuation, the dispersion and damping of uncoupled helicon waves, and the helicon-acoustic interaction are then analyzed in turn. Numerical solutions of the helicon dispersion relation are presented. The dispersion curve displays a branching in the absorption-edge region. A simple analytic treatment of the relaxation-time and effective-mass dependence of the helicon-acoustic interaction is given. The interaction near and in the absorption-edge region is investigated numerically. A rather large effect of this interaction on the magnetoacoustic absorption of potassium in the edge region is found.

I. INTRODUCTION

IN recent years, the interaction of acoustic waves in metals and semiconductors with the particular magnetoplasma modes known as helicons has been of interest. Interaction between transverse ultrasound and helicons has been observed in potassium by Grimes and Buchsbaum[1] and Libchaber and Grimes.[2] Shilz[3] has

studied the interaction of helicons with both longitudinal and transverse ultrasound in lead telluride. Noteworthy theoretical treatments based on the free-electron model have been given by Langenberg and Bok[4] and Quinn and Rodriquez.[5,6]

The motivating interest behind the present investigation was to arrive at a convincing description of the role of band-structure effects in the magnetoacoustic interaction in metals. A general theory of the dynamics and transport properties of localized Bloch electrons subjected to perturbations with a wavelike character has

[1] C. C. Grimes and S. J. Buchsbaum, Phys. Rev. Letters **12**, 357 (1964).

[2] A. Libchaber and C. C. Grimes, Phys. Rev. **178**, 1145 (1969).

[3] W. Shilz, Phys. Rev. Letters **20**, 104 (1968).

[4] D. N. Langenberg and J. Bok, Phys. Rev. Letters **11**, 549 (1963).

[5] J. J. Quinn and S. Rodriguez, Phys. Rev. Letters **11**, 552 (1963).

[6] J. J. Quinn and S. Rodriguez, Phys. Rev. **133**, A1589 (1964).